

FEL OPERATION WITH THE SUPERCONDUCTING RF PHOTO GUN AT ELBE

J. Teichert^{1#}, A. Arnold¹, H. Büttig¹, M. Justus¹, T. Kamps², P. Lu^{1,3}, P. Michel¹, U. Lehnert¹,
P. Murcek¹, J. Rudolph², R. Schurig¹, W. Seidel¹, H. Vennekate^{1,3}, R. Xiang¹, I. Will⁴,

¹Helmholtz-Zentrum Dresden-Rossendorf, Germany,

²Helmholtz-Zentrum Berlin, Germany,

³Technische Universität Dresden, Germany,

⁴Max-Born-Institut, Berlin, Germany

Abstract

The superconducting RF photoinjector (SRF gun) operating with a 3½-cell niobium cavity and Cs₂Te photocathodes is installed at the ELBE radiation center. Since 2012 a new UV driver laser system developed by MBI has been installed for the SRF gun. It delivers CW or burst mode pulses with 13 MHz repetition rate or with reduced rates of 500, 200, and 100 kHz at an average UV laser power of about 1 W. The new laser allows the gun to serve as a driver for the infrared FELs at ELBE. In the first successful experiment a 260 μA beam with 3.3 MeV from the SRF gun was injected into the ELBE linac, further accelerated, and then guided to the FEL. First lasing was achieved at 41 μm wavelength. The spectrum, detuning curve and further parameters were measured.

INTRODUCTION

High-brightness electron sources for CW operation with megahertz pulse repetition rates and bunch charges up to 1 nC are still a topic for research and development. One promising approach is a superconducting radio-frequency photoelectron injector (SRF gun), which is able to combine the high brightness of normal conducting RF photo guns with the advantages of superconducting RF, i.e. low RF losses and CW operation. At present, R&D programs are conducted in a growing number of institutes and companies. (See Ref. [1].)

Details of the ELBE SRF gun design have been published in [2]. The SRF gun is able to inject an electron beam into the ELBE linac using a dogleg-like connection beamline since 2010. In 2012 a new ultraviolet driver laser for the SRF gun was installed which had been developed at the MBI, Berlin. This laser delivers pulses with 13 MHz (ELBE FEL mode) as well as lower repetition rates (500, 250, 100 kHz) for high-charge operation. The new laser allows applying the SRF gun for the FEL operation at ELBE, and in this paper we will report on the first successful attempt.

SRF GUN

Photocathodes and Laser

The SRF gun has been designed for the use of high quantum efficiency (QE), semiconductor photocathodes.

#j.teichert@hzdr.de

Up to now Cs₂Te has been used. This material has both high QE and robustness against vacuum deterioration. The photocathode plug with a diameter of 10 mm was made of Mo polished to a roughness of 8 nm. A Cs₂Te photo emission layer of 4 mm diameter was deposited on top by successive evaporation of Te and Cs in an ultra-high-vacuum preparation system [3]. The currently used photocathode was prepared 12 months ago with a fresh QE of 8.5 %, while a recent measurement has shown 0.6%. The QE decrease happened during storage in the first weeks. Inserted in the SRF gun, the experience is that the photocathodes have lifetimes of months and relatively stable QE. For the present photocathode the total charge extracted is 265 C at an average current up to 0.5 mA.

The driver laser consists of a Nd:glass oscillator at 52 MHz, a pulse picker generating the 13 MHz with an electro-optical modulator, a fiber-laser preamplifier, a multipass amplifier, and a frequency conversion stage with lithium triborate (LBO) and beta-barium borate (BBO) crystals. The UV laser pulse had a Gaussian shape in time with a FWHM value of about 3 ps. The transverse profile can be shaped with a variable aperture. Here the aperture was completely opened in order to obtain maximum laser pulse energy. Thus, the transverse profile was also Gaussian with 1.2 mm FWHM. The UV laser power on the laser table was measured as 600 mW. Considering the transportation losses of 50 %, the laser pulse energy at the photocathode was about 23 nJ. The laser spot was centred on the photocathode and the laser parameters were optimized to maximize the electron current. A value of 260 μA which corresponds to a bunch charge of 20 pC was obtained und held stable during the whole beam time.

Cavity Performance

The cavity performance, i.e. the intrinsic quality factor Q_0 versus the peak electric field, has been measured regularly since the commissioning of the gun in 2007. Fig. 1 shows some results of these measurements. The practical limitation for the peak field value of the acceleration field is the strong field emission. The acceptable heat loss is about 30 W. From 2007 until 2011 the values for the peak fields were 16 M/m in CW and 21.5 MV/m for pulsed RF. A temporary improvement was obtained by high power processing (HPP) of the cavity. In autumn 2011 a number of photocathodes were exchanged within a short time for testing new designs and

materials, as well as vacuum repair work was carried out at the beamline near the SRF gun. The measurement carried out afterwards (December 2011) showed a performance decrease of 12%. But no further deterioration has been observed up to the present. Our experience is that the photocathode operation does not alter the gun cavity performance, but the frequent cathode exchange is a critical issue.

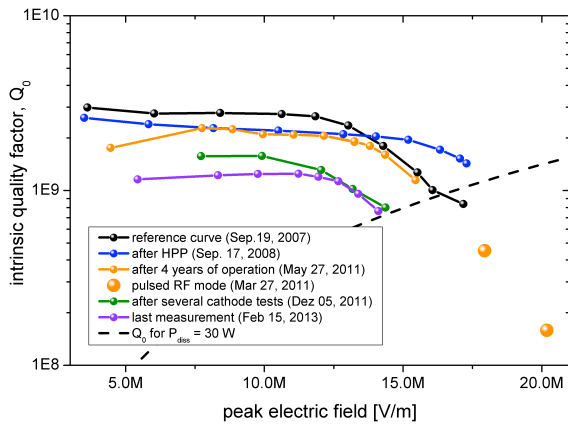


Figure 1: Measurement of the cavity performance.

Operational Parameters and Electron Beam

The SRF gun was operated with pulsed RF. This allowed a higher acceleration gradient at low RF losses into the helium path and thus a more stable operation at higher exit energy. The RF pulse consisted of a ramp-up time with increasing gradient and a macropulse time, in which the gradient and phase is stabilized and the beam can be produced. These times were fixed to 12 ms and 6 ms, respectively. The repetition period of the RF pulses was chosen to be 800 ms. The acceleration gradient was $E_{acc} = 6.6$ MV/m which corresponds to a peak field of $E_{peak} = 18$ MV/m ($E_{peak} = 2.7 * E_{acc}$) and yields 3.3 MeV kinetic energy at the gun exit.

During the ramp-up time of the RF, multipacting appeared in the coaxial channel formed by the hole in the backplane of the half-cell and the photocathode. To suppress this effect, a distinct DC voltage is applied to the photo cathode. For pulsed operation this voltage has to be present all the time and was chosen to be -5.3 kV with respect to the grounded cavity.

The driver laser phase, which determines the time when the laser pulse hits the cathode, was set to -5° . A typical laser phase scan measured with the same gun parameters but with slightly lower beam current is shown in Fig. 2. Due to the cathode's DC field, electron beam emission starts at negative laser phases. The phase window with nearly constant beam current reaches up to 60° . The upper limit is due to phase mismatch of the bunch in the full cavity cells, i.e. the electrons start too late to be accelerated. In general, the beam quality is better for a small laser phase. As an example, the dependences of the beam energy and energy spread on the laser phase are

presented in Fig. 2. An earlier measurement using the slit scan method delivered a value of $1 \text{ mm} \cdot \text{mrad}$ for the normalized rms emittance. The relevant parameters like acceleration gradient, laser phase, and laser spot size where the same as in the present gun setup.

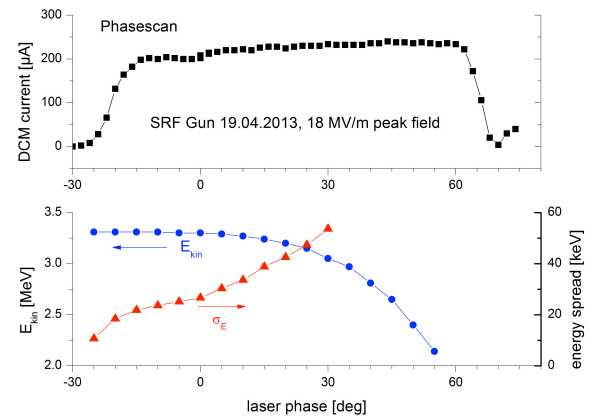


Figure 2: Laser phase scan: FC current, energy, and energy spread.

LINAC

The beamline layout with the SRF gun, dogleg, accelerator, S-bend, and FEL is presented in Fig. 3. Starting with 3.3 MeV at the SRF gun exit, the electrons were accelerated to 16 MeV in the first ELBE module (cavities C1 and C2) and up to the final energy of 27.9 MeV in the second ELBE module (cavities C3 and C4). View-screens were utilized for steering the beam exactly. At a number of places stripline monitors detected the beam current and helped to sustain full transmission. A loss-free and achromatic beam transport in the dogleg section was essential for the success. After achieving that, the phases of the linac cavities were matched and the final energy adjusted. Finally, the steering and focusing in the S-bend and undulator section were carried out.

The energy chirp of the electron bunch behind the gun and the dogleg was negative, i.e. the electrons in the head of the bunch had higher energy than those in the tail. In the first cavity C1 this correlated energy spread was compensated by setting the RF phase about 20° off crest. The following cavities C2 to C4 were operated on-crest. The magnetic bunch compressor (chicane) between the two ELBE modules was not used.

The S-band from the switching magnet to the undulator U100 has a positive momentum compaction coefficient of $R56 = 93$ mm. (In the convention used here a chicane has a negative sign, i.e. $R56 < 0$) Thus, the S-bend could shorten the bunch in case it had a negative energy chirp. But due to the compensation with cavity C1, the bunch length was unchanged and had the same value as initially created in the SRF gun.

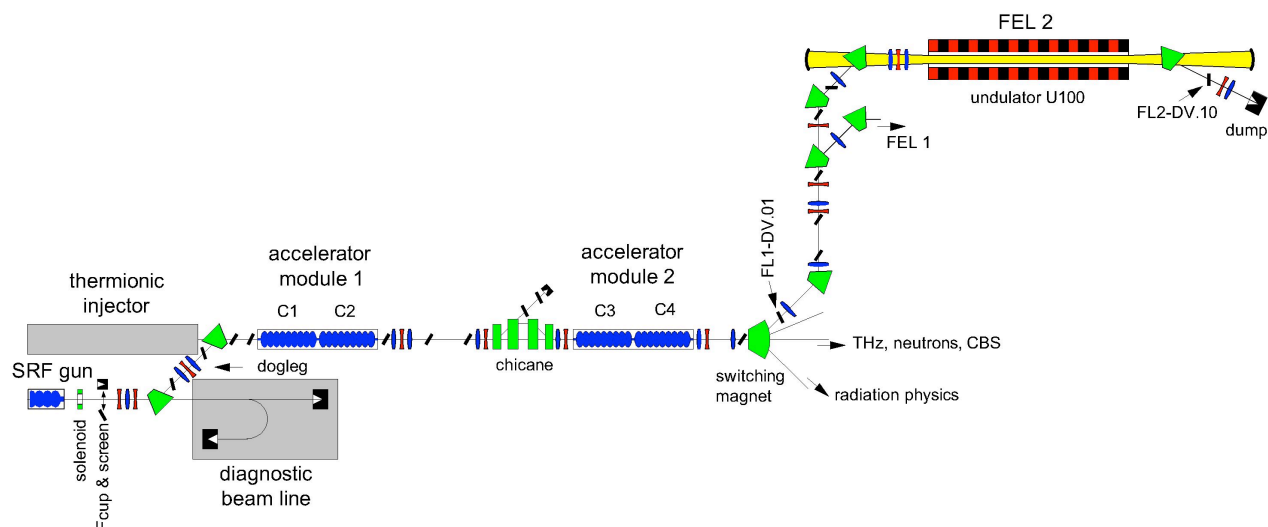


Figure 3: ELBE beamline for FEL operation with SRF gun.

The longitudinal phase space parameters in the linear approximation were measured by applying the phase scan technique, which is described in [4]. This means the RF phase of cavity C4 was varied while the beam energy spectrum was measured using the dipole magnet downstream the ELBE module 2 and the first screen right behind it (screen FL1 DV.01 in Fig. 3).

As mentioned above, the cavities C2 to C4 were on crest in this particular accelerator setup. Therefore, they did not alter the longitudinal phase space and C4 could be used for the measurement. In a second measurement series, the C1 phase was set on crest too. In this case the data delivers the phase space as produced by the SRF gun itself. In Fig. 4, it can be seen that the energy correlation was slightly overcompensated in the lasing setting giving a correlation parameter of 0.19. The bunches delivered by the gun itself had a correlated energy spread of 20 keV and a correlation parameter of 0.58. The rms bunch length was measured to 1.6 ps with good agreement between both measurements. For the rms longitudinal emittance with a value of about 40 keV·ps, the difference is larger and mainly caused by the simple measurement setup with a high background.

FAR-IR FEL

Undulator, Optical Cavity, and Diagnostics

The U100 FEL for radiation in the far infrared range from 18 to 250 μm is based on a SmCo hybrid undulator which is composed of 38 magnet periods each 100 mm long. The K_{rms} can be adjusted from 0.3 to 2.7, which corresponds to gaps of 85 to 24 mm. The FEL is equipped with switchable outcoupling mirrors (three different hole diameters of 2, 4.5, and 7 mm). In order to obtain sufficient magnetic fields in the undulator, the gap and consequently the place for the optical mode has to be adequately small. Therefore, the U100 FEL is equipped with a partial parallel-plate waveguide with 10 mm height. The horizontal size is wide enough to allow free

propagation. The waveguide spans from the undulator entrance to the downstream mirror. In the remaining part of the optical cavity the optical mode propagates freely. The mirrors are toroidal at the free propagation side and cylindrical at the waveguide side. The infrared light produced by the FEL is guided into the diagnostics room. There are several detectors, a multichannel spectrometer, and two power meters for intensity measurements. The FEL has been in routine operation at ELBE since 2006 using the thermionic injector [5].

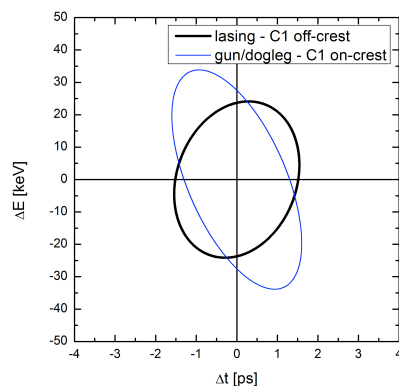


Figure 4: Longitudinal phase space ellipses for the lasing setting with nearly compensated correlated energy spread (C1 off-crest), and in the ellipse as produced by the gun (C1 on-crest).

Lasing and Results

For the experiment reported here, the undulator gap was set to produce radiation of 41.5 μm wavelength, which corresponds to a gap of 50.8 mm. Later, the gap was changed to 46.2 mm. The mirror with the smallest out-coupling hole (2 mm) was chosen. The adjustment of the optical mirror axis was checked and the electron beam guided through the undulator by means of the OTR screens. Finally, the optical cavity length was scanned. To

find the onset of lasing, the infrared pyroelectric detector signal and the electron beam spot image on the screen in the dispersive section behind the deflecting magnet (screen FL2-DV.10 in Fig. 3) were observed. Here a distinct increase of the electron energy spread was expected.

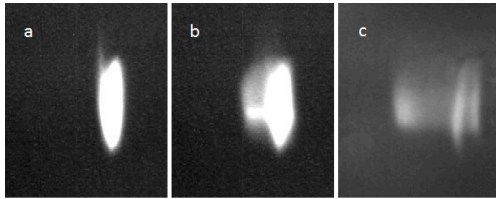


Figure 5: Beam spot in the dispersive section behind the FEL: (a) before lasing, (b) first lasing, (c) lasing with optimized beam transport in undulator.

Fig. 5 shows the OTR screen pictures of the electron beam before and during FEL lasing with the expected increased energy width. The first measured detuning curve of the FEL is shown in Fig. 6 while the infrared spectrum is presented in Fig. 7. The width of the peak was measured to be 1 μm FWHM.

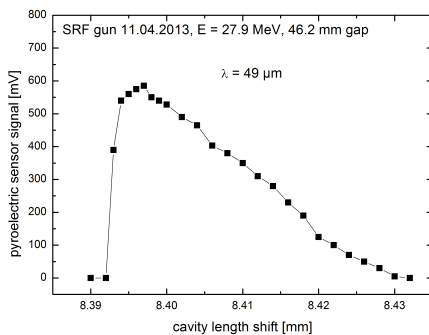


Figure 6: Measured FEL detuning curve for 49 μm wavelength. The length scale is the relative downstream mirror position. Zero detuning length is nearly located at the left-side slope of the curve.

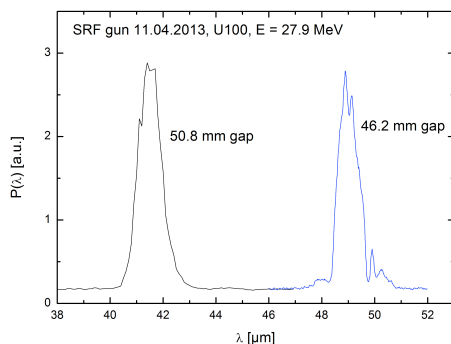


Figure 7: First measured FEL infrared spectra.

The stability of the FEL output power was measured over an adequate time. The result which delivers an amplitude variance value of 12 %, is similar to the one for FEL operation with the thermionic injector.

SUMMARY

Since the operation of a FEL requires a comparably high level of beam quality especially with respect to all kinds of stabilities like energy, bunch charge, transverse and longitudinal beam parameters, the successful lasing with the SRF gun represents an important milestone and confirms the design concept for this gun.

The long-term experience with Cs_2Te is promising. The operational lifetime is months and average currents up to 0.5 mA have been produced. For the cavity performance we have not seen any degradation which is due to the operation of the gun. A decrease of 12 % in cavity performance since 2007 is likely caused by cathode exchange or beamline vacuum work.

ACKNOWLEDGEMENTS

We would like to thank the whole ELBE team for their help and assistance with this project. The work is supported by the European under the FP7 programme (EuCARD, contract number 227579, and LA³NET, contract number 289191), and by the German Federal Ministry of Education and Research grant 05ES4BR1/8.

REFERENCES

- [1] A. Arnold and J. Teichert, "Overview on superconducting photoinjectors," *Phys. Rev. ST Accel. Beams* 14 (2011) 024801.
- [2] A. Arnold et al., "Development of a superconducting radio frequency photoelectron injector," *Nucl. Instr. and Meth. A* 577 (2007) 440.
- [3] R. Xiang et al., "Research activities on photocathodes for HZDR SRF gun," IPAC'12, New Orleans, USA, June 2012, p. 1524 (2012); <http://www.JACoW.org>
- [4] D.H. Dowell et al., "Longitudinal emittance measurements at the SLAC gun test facility," *Nucl. Instr. and Meth. A* 507 (2003) 331.
- [5] W. Seidel et al., "Three years of CW operation at FELBE – experiences and applications," FEL'08, Gyeongju, Korea, August 2008, p. 382 (2008); <http://www.JACoW.org>